MULTI-TEMPORAL MONITORING OF SLOW MOVING LANDSLIDES IN SOUTH PINDUS MOUNTAIN RANGE, CREECE

Christina Psychogyiou [(1)], Ioannis Papoutsis [(1)], Charalambos Kontoes [(1)], Eleftheria Poyiadji[(2)], Natalia Spanou[(2)], Nikolaos Klimis[(3)]

[(1)] *National Observatory of Athens, Institute of Space Applications and Remote Sensing, Athens, Greece, cpsychogyiou@noa.gr*
[(2)] *Institute of Geology and Mineral Exploration, Athens, Greece, kynpo@igme.gr*
[(3)] *Section of Geotechnical Engineering, Department of Civil Engineering, Democritus University of Thrace, Xanthi, Greece, nklimis@civil.duth.gr*

ABSTRACT

The high frequency of landslide occurrences in Central and Western Greece, part of the Pindus mountain range, is now approached by exploiting the high temporal sampling rate of historical ERS-1/2 and ENVISAT SAR imagery in combination with the Multi Temporal Interferometry (MTI) technique. An existing well-established ground truth dataset is updated and enriched with the diachronic MTI results. Critical areas prone to slide are evaluated through susceptibility assessment and mapping taking into consideration the challenging environmental factors which dominate at the area of interest. A set of supplementary interesting geophysical and structural MTI detections at the region of analysis are additionally discussed.

1. INTRODUCTION

The area selected as case study is located at Central and Western Greece, where the Southern part of mountain range Pindus, the "backbone" of Greece's mainland, lies. The area of interest extends over 4000km^2 and covers two prefectures, those of Aitolia-Acarnania and Evritania. High altitudes, steep slopes, flysch formations and high precipitation levels dominate at that region and they often enhance the occurrence of instability phenomena. The region has experienced numerous landslide events raising concerns to local authorities and national institutes.

The potential of exploiting satellite remote sensing data for the identification and mapping of small-scale slope failures has been improved substantially over the last decade, [1]. This was prompted by the availability of sufficiently long series of radar images acquired in particular by the European Space Agency (ESA), the development of the Multi Temporal Interferometry (MTI) techniques and the presentation of several successful examples of MTI applications to landslide investigations (e.g. [2]; [3]; [5]), [4]. The interpretation of the exact geotechnical significance of small, radar sensed ground surface deformation is challenging, especially where ground truth is lacking, [4].

The valuable tool of Multi Temporal Interferometry technique has been implemented for the periods 1992-2000 and 2003-2010 using ERS1/2 and ENVISAT datasets, primarily for detecting extremely to very slow moving landslides (according to velocity scale proposed by IGUS/WGL, 1995). The availability of pre-existing landslide inventory at the region of interest provided by the Institute of Geology and Mineral Exploration - IGME-GR (Greek Geological Survey) permits the spatial correlation of the MTI results with ground truth observations leading to an updated inventory and to susceptibility statistical assessment and mapping. Additionally, the wide spatial coverage of the processed frame has also allowed the recognition of subsidence phenomena, tectonic deformation rates and settlements on infrastructures of economic and social impact at the region of interest.
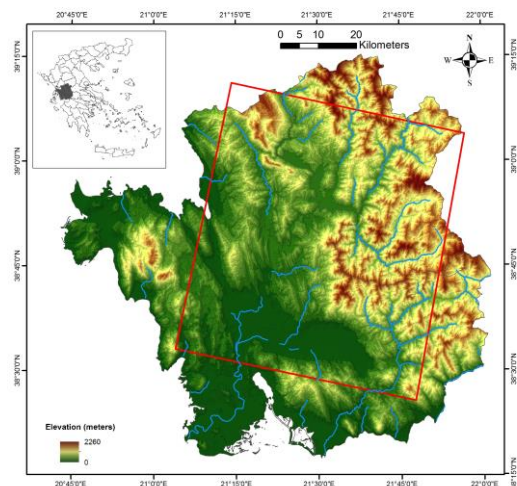

Figure 1. The area of interest marked in red rectangle on a background morphology setting map

2. TECTONIC AND GEOLOGICAL SETTING

The investigated region belongs to Gavrovo-Tripolitza and Pindus 'isopic' zones of the External Hellenides and partly to Ioanian zone. The Pindus Zone is formed by Pelagic sediments and is overthrusted over the neighbouring zone of Gavrovo. Jurassic and Cretaceous carbonates are common in the Pindus thrust zone, where ophiolithes appear with shales and radiolarian cherts, then flysch deposits overthrusted them. In this zone the plastic tectonic formation of foldings dominates such as

overthrusts and tectonic nappes, [6].

The Gavrovo - Tripolitsa Zone is formed out of neritic sedimental deposits which have been overlaid the meiogeoanticline ridge. The age of these sedimental deposits belongs to the Cretaceous, Mid-Eocene period. On the top of the above mentioned sediments, flysch lays belonging to the Upper Eocene and Oligocene. The tectonic of this zone is characterized by a sequence of anticlines and synclines with many faults and strong displacements, [6].

The Ionian Zone consists out of sediments belonging to the Pelagic phase, while weak overthrusts directed westwards characterize the tectonic of the zone, [6].
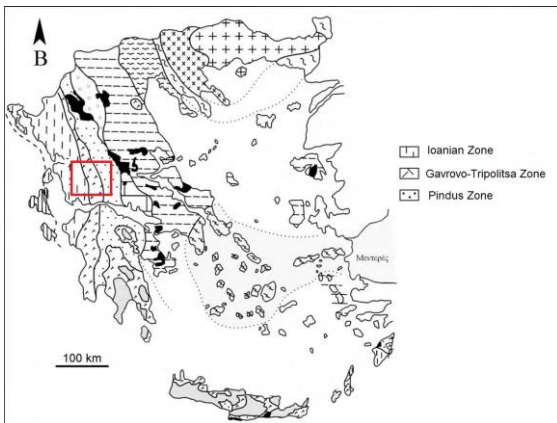

Figure 2. Isopic zones of the area of interest marked in red with the corresponding legend, [7].

The regional morphology is dominated by mountainous topography characterized by high relief reaching 2000m a.s.l., significant hydrographic features and high precipitation levels which often lead to phenomena of instability, mainly at the mantle loose materials and fragmentation zones.

At the southern part of the frame, Trichonis Lake is the largest natural lake in Greek territory with 93km^2 of surficial extent. Trichonis graben is a well-known Quaternary structure of western Greece that strikes WNW–ESE. The Trichonis fault, is the major, topography controlling normal fault, is north-dipping and bounds the south shore of the lake [8] where it is locally buried under Pleistocene deposits and thick alluvial cones, [9].

At the West of the frame, the sinistral strike-slip faults connect the Gulf of Amvrakikos and the Gulf of Patras and form the Amphilochia–Katouna–Aitoliko Fault Zone, representing a subsiding basin, [9].
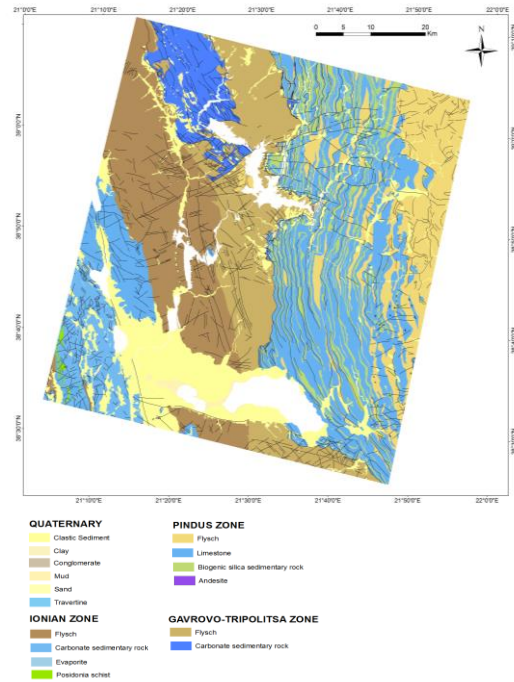

Figure 3. Regional Geology map, [10]

3. METHODOLOGY WORKFLOW

Landslide quantitative hazard and risk assessment requires a complete landslide inventory. Landslide inventory is the most important input layer, as it gives an insight at the location of past landslide occurrences, as well as their failure mechanisms, causal factors, frequency of occurrence, volumes and the damage that has been caused, [11].

Towards an updated landslide inventory, remote-sensing plays a key role for landslide identification, monitoring and mapping. Landslide boundaries confirmation and updating, new detections and landslide activity evaluation are achieved due to wide area coverage, non-invasiveness, and cost-effectiveness of remotely sensed data, [12].

As presented in the workflow graph (Fig. 5), the current study couples pre-existing landslide inventory of field investigations from 1965 to 2010 (Fig. 4) with Multi Temporal Interferometry technique by exploiting ERS1/2 and ENVISAT historical time series dataset, in terms of displacements and average velocities measurements. The pre-existing inventory is accompanied with a set of attributes for each recorded event, such as landslide location, year and season of occurrence, previous activation, geological formation, implications provoked to local infrastructures, landslide movement type and depth characterization. The correlation of the above mentioned layers are integrated with the aid of conventional visual photo interpretation of high resolution imagery regarding the recognition of scatterers inside or close to existing records and new landslide detections where there was no previous

evidence on landslide movements, depending also on geomorphological evidences and indicators (e.g. anomalies in vegetation coverage), [13].
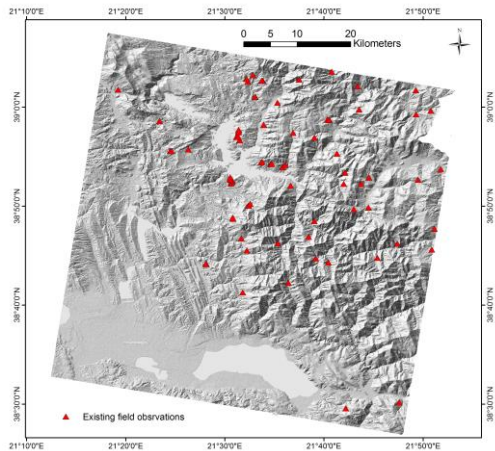

Figure 4. Pre-existing landslide field recordings in red points

In addition to landslide inventory, predisposing factors emerge as a crucial information layer so that to establish the link of the landslide spatial distribution with the topographic, geological, hydrological, and geomorphological settings of the area. So, thematic maps describing environmental factors which influence instabilities were generated. Elevation, slope inclination, aspect and convexity maps are derived from DEM with resolution of 5m×5m provided by the National Cadastral and Mapping Agency SA. Geological map was also taken into account.

A detailed landslide inventory is the principal for a quantitative approach to landslide susceptibility assessment which defines the spatial probability of landslide occurrence. A landslide susceptibility map subdivides the terrain into zones with different spatial likelihoods of occurrence in terms of identifying the most probable initiation areas, [11].

The data-driven, statistical, bivariate method of Information value was chosen for the landslide susceptibility assessment, in which the combination of factors that have triggered landslides in the past are evaluated statistically, and quantitative predictions are made for current non-landslide affected areas with similar geological, topographical and land-cover conditions, according to the assumption that past conditions are indicative of future conditions, [11].

The employed statistical approach is appropriate for susceptibility assessment at regional working scale of 1:20,000 and it was applied by using the software package ArcGIS platform by Esri GIS, for grid units of 20m.

Fig. 5 presents the workflow of the methodology followed for the development of a fully updated landslide inventory map and the statistical approach for the susceptibility assessment.
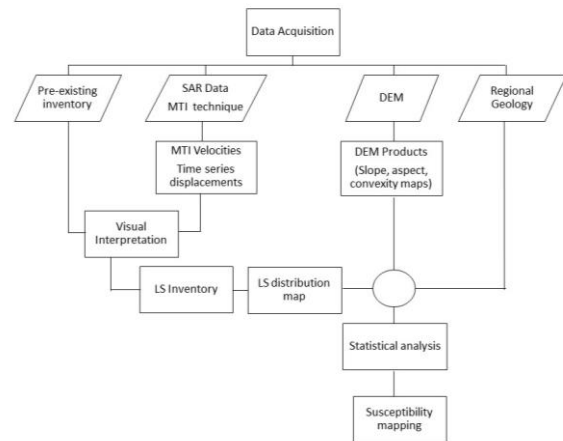

Figure 5. Workflow towards landslide inventory and susceptibility assessment

4. MTI PROCESSING

Pre-processing investigation showed that layover and shadowing image distortions were minimized for the descending satellite trajectory and the track 50 was chosen as the most suitable for the analysis, so that to capture as many as possible slopes.

Time series analysis is conducted by processing 53 SAR images of ERS1/2 sensors and 23 images of ENVISAT sensor, monitoring extremely to very slow moving landslides for the periods 1992-2000 and 2003-2010, respectively. The open source software package StaMPS [14] was used for the SAR images processing, by incorporating Persistent Scatterers [15] and Small Baselines [16], plus the option to combine both techniques [17]. The PS approach identified bare soil outcrops, semi-urban areas and infrastructures, whereas the SBAS approach provided additional coherent pixels in semi-vegetated and agricultural lands. Table 1 presents explicitly the dataset used and the post-processing information.

Table 1. Characteristics of the satellites used and post-processing information

Satellite	ERS 1/2	ENVISAT
Band	C	C
Geometry	Descending	Descending
Temporal Range	1992-2000	2003-2010
Nº Scenes	53	23
Nº of Interf. pairs	201	54
PS/km^2	31	31
LOS vel. range (mm/yr)	[-15 +5]	[-10 +5]

5. RESULTS ON LANDSLIDES MONITORING

Fig. 6 and 7 demonstrate the mean velocity values along the line of sight for the periods 1992-2000 and 2003-2010 for ERS1/2 and ENVISAT sensors. As reference area was set the city of Agrinio, located to the West of Trichonis Lake.

At the perimeter area of Kremasta Lake, the largest artificial lake in Greece, high LOS velocities up to 15mm/yr away from the satellite are captured, indicating landslide phenomena.

The behaviour of slope-forming materials at that region can be characterized by poor mechanical properties, as the surficial soil masses consist of aggregate of minerals and rock fragments.

Shallow mud and debris landslides are often triggered at the area studied by high precipitation levels and hydrological conditions along the slopes of the dense stream network, where loose materials dominate. The MTI displacement rates detect post-failure ground movements and ongoing erosion processes. At higher altitudes, MTI technique identifies creep movements along slopes with steep gradients at bare rock outcrops or soil scarps where vegetation interruption allows scatterers detection.
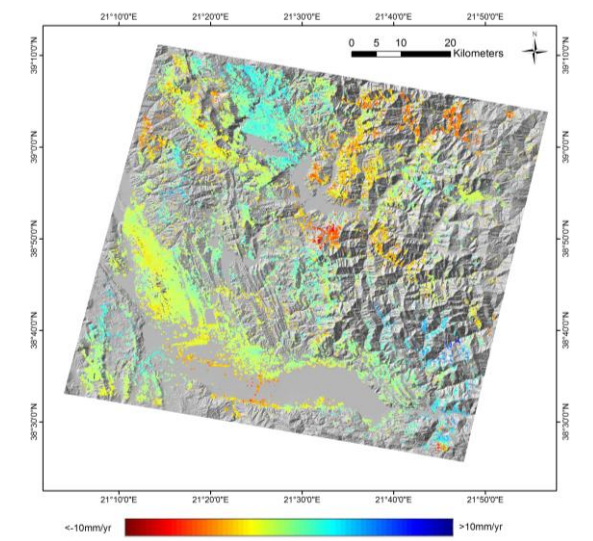

Figure 6. ERS 1/2 LOS mean velocities

In Fig. 8, the landslide distribution map presents active landslides detected by MTI technique and characterized by velocity values higher than 2mm/yr away from the satellite (excluding tectonic deformations and potential noisy results) integrated with existing in situ surveying records. In total, 600 landslide polygons are taken into consideration as the examining population for the susceptibility assessment, using half of it as training set and the rest as validation set.
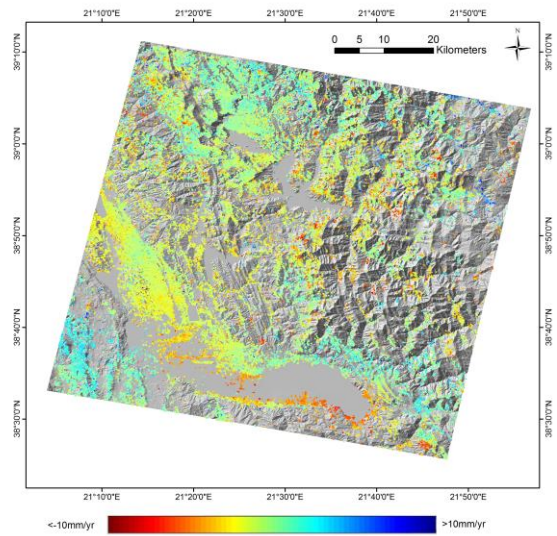

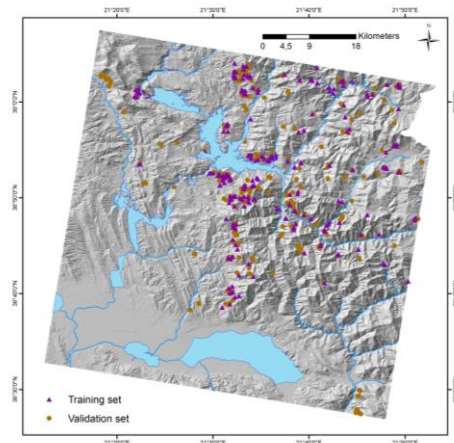*Figure 7. ENVISAT LOS mean velocities*

Figure 8. Landslide distribution map as location points

5.1 Landslide susceptibility assessment

The principal idea of the applied susceptibility assessment approach is the attribution of weighted values on each individual factor based on the overlaying of the past landslide occurrence distribution map.

The modeling technique applied for geofactor weighting is known as the Information Value method. In this approach, an information value I is calculated as numerical weight for each geofactor attribute $A_{(i)}$. The value of $I_{A(i)}$ describes the contribution of $A_{(i)}$ to former landslide occurrence and can be expressed in terms of frequency statistics as follows [18]:

$$I_{A(i)} = ln \frac{N_{A(i)} / S_{A(i)}}{N/S} \quad (i = 1,2,3, ..., n) \qquad (1)$$

where $N_{A(i)}$ is the number of landslides in attribute class $A_{(i)}$, N is the number of landslides in the entire territory,

$S_{A(i)}$ is the total area of attribute class $A_{(i)}$, and S is the total area of the entire territory. In consequence, attributes having positive values of $I_{A(i)}$ are likely to promote instability, while otherwise their influence can be interpreted as negative. The geofactor weights are used to calculate the final susceptibility index SI(x) that describes the landslide predisposition of the basic mapping unit. SI(x) is defined as the sum of all values of $I_{A(i)}$ in a defined grid cell of 20 m and can be computed as follows:

$$SI_{(x)} = \sum ln \frac{N_{A(i)}/S_{A(i)}}{N/S} \quad (i = 1,2,3,...,n) \quad (2)$$
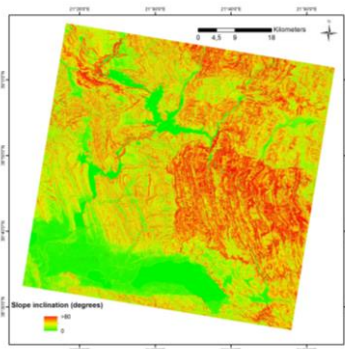

Figure 9. Slope inclination map

As emerged from the statistical susceptibility assessment, geology and slope inclination layers constitute the most influential factors for the characterization of highly susceptible initiation areas.

The landslide susceptibility map (Fig. 12) mainly follows the pattern of the geology and slope inclination classifications, by attributing very high susceptibility to areas located at Pindus zone. Limestone, biogenic silica sedimentary rocks and flysch layers override one another in alternating sequence and in combination with steep slope gradient of over 60 degrees at high relief (600-1000m) generate a favorable setting for landslide initiation.

Flysch formation class of Gavrovo-Tripolitsa zone is categorized as highly susceptible since weak geotechnical properties of reduced shear strength govern the slope materials.

Convex slopes are more prone to landslides than concave, because of the increased tensional forces due to the outward bend which enhance downward movements. Slope units facing West and SW are characterized by high landslide geofactor as their vertical orientation to West and SW air masses movement results to intense precipitation levels triggering instabilities.
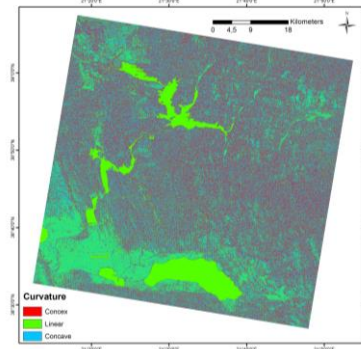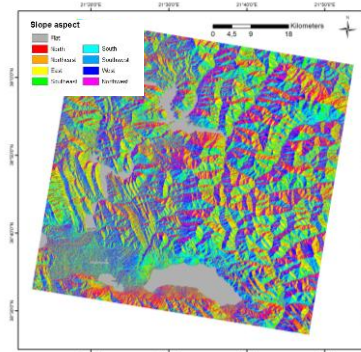

Figure 10. Curvature map
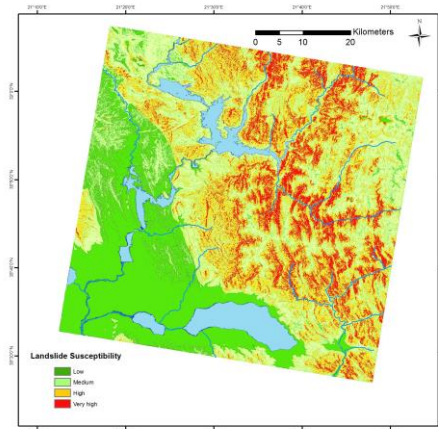

Figure 11. Slope aspect map

Figure 12. Susceptibility map

.
The performance of the statistical model is evaluated using areas under curve (AUC). The success rate was calculated comparing the training set with the susceptibility map. The predictive rate was generated using the validation set which was not used to build the model. The AUC values demonstrate reasonably good accuracy for the study area at regional scale with success and prediction accuracy of 77% and 76.5%, respectively.
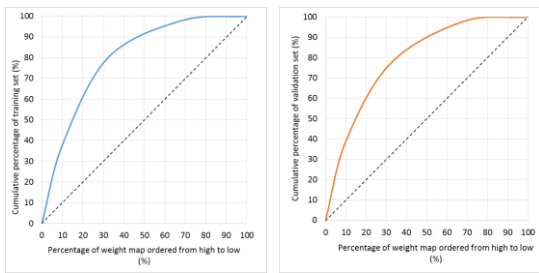
Figure 13. Success rate (left) and prediction rate (right) of the statistical model

6. MTI COMPLEMENTARY RESULTS

6.1 MTI results on Trichonis Lake

At ERS1/2 velocity results (Fig. 6), it is worth noting the negative displacement rates along the perimeter and Western shore of Trichonis Lake indicating subsidence phenomena with the velocity reaching -5.5mm/yr.

The observations can be associated with the limestone masses falling down into the existing underground caverns which form a quite extensive Carstic network, due to the corrosive and solvent action of the water, resulting thus to the change of the regional morphology, [6].

According to Corine 2000, the area is occupied by permanently irrigated land and complex cultivation patterns. It is generally observed that during the 6 month period of April to September, 40% of the total annual outflows of the Trichonis Lake are pumped for agricultural purposes which results in very rapid water level drops more than 60 cm (mainly May–September) causing extended drought in the wetland area, [19].

The pattern of subsidence at this region remains also evident at the ENVISAT results (Fig. 7), but with an increasing rate at the SE shore of the Trichonis Lake. On 8 April 2007 an earthquake swarm burst near the SE bank of Lake Trichonis. The three strongest events of the swarm occurred on April 10th with moderate magnitudes ranging from Mw 5.0 to Mw 5.2. The most serious damage was reported in the village Thermon 5 km to the NE of the earthquake epicentres. The deforming area of the Eastern area of the Trichonis Lake due to the 2007 earthquake swarm revealed a NW-SE striking structure that dips to the NE. The structure is located at the eastern of Trichonis fault and strikes at a ~45° angle to it, (Fig. 15), [9].

Fig. 14 presents the time series displacement graph for scatterers detected by ENVISAT data processing at the Eastern shore of Trichonis Lake. It is observed that in between January 2007 and March 2008, a significant subsidence is recorded exceeding 3cm, which may infer the earthquake swarm of April 2007, compared to the gradual subsidence trend displayed from May 2003 till January 2007.
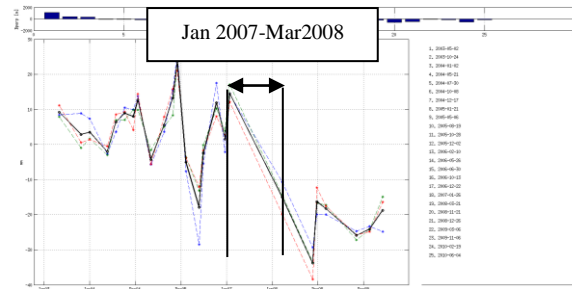

Figure 14. PS time-series displacements at the Eastern shore of Trichonis Lake after ENVISAT data processing

6.2 MTI results on Amphilochia tectonics

At the Western part of the frame, the opposite displacement rate signs for both ERS1/2 and ENVISAT sets are attributed to the discontinuity of left lateral strike slip fault system of Amphilochia - Katouna corresponding to an N-NW trending valley. The fault zone forms the natural boundary between the crustal fragments of Karpenissi and Akarnania at E-W and links the Gulf of Amvrakikos with the Gulf of Corinth at N-S, [20].
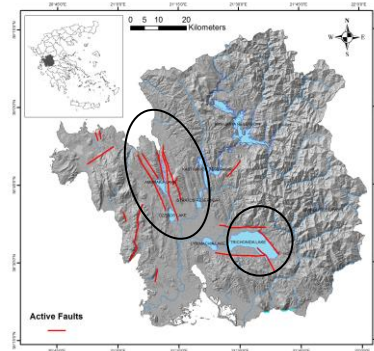

Figure 15. Active fault zones map indicating Amphilochia fault zone (upper left) and Trichonis structure (low right)

6.3 MTI results on earth dams settlements

The area of interest is characterized by a complex river network, with the river Achelous being the most important aquifer feature of the Western Greece. Achelous River begins at 2000m a.s.l. Lakmos springs in the mountain Pindus range, extends for 220km along SW direction and empties into Ionian Sea.

At the middle of 20th century, Kremasta, Kastraki and Stratos dams were constructed successively along Achelous watershed for hydropower plant exploitation purposes. Kremasta earth-fill dam is one of the highest dams in Europe (160.3m). MTI technique indicated settlements at the crest and at the downstream face of the Kremasta embankment dam (Fig. 17).

Geodetic monitoring records for the period 1966-2003

have demonstrated long-term deformations of the crest reaching up to 800mm. Creep and/or secondary consolidation of clay, reservoir level fluctuations and rainfall are the main three possible mechanisms affecting the crest settlements, [21].

Kastraki earth-fill dam is the second Achelous flow barrier to the way downstream. MTI results reveal settlement patterns (Fig. 18) of smaller scale compared to Kremasta Dam, deformation which is also confirmed by geodetic measurements reaching 160mm for monitoring period of 1963-2003, [21].
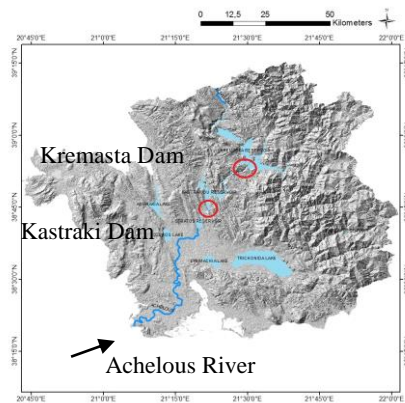

Figure 16. Achelous river watershed and the two earth dams' locations marked in red circles
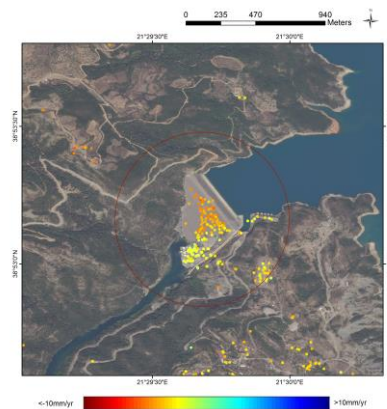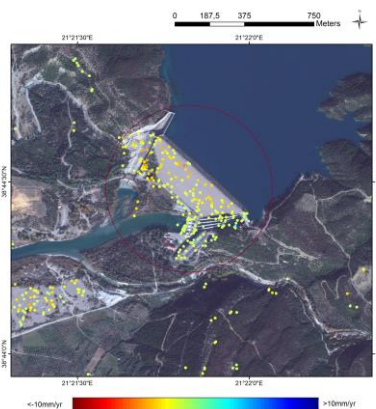

Figure 17. Settlements at Kremasta earth dam

Figure 18. Settlements at Kastraki earth dam

7. CONCLUSIONS

The present work aims at the improvement of the background knowledge and the demand for long term monitoring of slow moving landslides at the wide area of South Pindus mountain range at Central and Western Greece. The challenge to follow small scale slow moving landslides with high spatial frequency at a particular geological, morphological and densely vegetated setting triggered the need for combined approach of Multi Temporal Interferometry (MTI) technique with pre-existing field observations at the area of interest. The exploitation of ERS 1/2 and ENVISAT historical datasets in terms of velocities, reaching up to 15mm/yr along line of sight away from the satellite, supports the updating of the pre-existing inventory affirming successfully past recorded landslides hot spots as well as the recognition of new. Based on the integrated landslide dataset and the environmental factors of the area, the statistical bivariate approach of Information Value was implemented towards landslide susceptibility assessment at regional scale. Flysch and sedimentary rock formations of Pindus and Gavrovo-Tripolitsa zones proved to be the most susceptible in combination with steep slope gradients that dominate the area of interest. Convexity and W - SW slope orientation increase the likelihood of instabilities.

Complementary to landslide monitoring, MTI results reveal interesting findings at the wide area of coverage. At Trichonis Lake, at the southern part of the studied frame, subsidence phenomena due to physical and anthropogenic processes are detected, as well as tectonic activity is captured during the 2007 earthquake swarm. Tectonic deformation of Amphilochia discontinuity fault zone is affirmed and structural settlements on two earth dams of vital significance for the area are observed.

As perspective work, field investigations will further reinforce the inventory with contemporary ground truth data. In addition, the implementation of a physically based model at regional scale will permit the correlation of MTI results with a geotechnical slope stability factor of safety approach. At crucial landslide spots, site specific analysis will employ a sophisticated finite elements model to simulate slope stability linked with precipitation and dynamic loading.

8. ACKNOWLDEDGMENTS

9. REFERENCES

1. Van Westen, C.J., Van Asche T.W.J. & Soeters, R. (2006). Landslide hazard and risk zonation-why is it so difficult?. *Bulletin of Engineering Geology and the Environment* 65: 167–184.

2. Colesanti, C., Ferretti, A., Novali, F., Prati, C. & Rocca, F. (2003a). SAR monitoring of progressive and seasonal ground deformation using the permanent scatterers technique. *IEEE Trans. Geosci. Remote Sens*. 41 (7), 1685–1700.

3. Hilley, G.E., Burgmann, R., Ferretti, A., Novali, F. & Rocca, F. (2004). Dynamics of slow-moving landslides from permanent scatterer analysis. *Science* 304, 1952–1955.

4. Colesanti, C. & Wasowski, J. (2006). Investigating landslides with space-borne Synthetic Aperture Radar (SAR) interferometry. *Engineering Geology* (88), 173–199.

5. Wasowski, J. & Bovenga, F. (2014). Investigating landslides and unstable slopes with Satellite Multi Temporal Interferometry: Current issues and future perspectives. *Engineering Geology* (174) pp. 103-138.

6. Delibasis, N. & Karydis, P. (1977). Recent earthquake activity in Trichonis region and its tectonic significance. *Ann. Geofis*. 30, 19 – 81.

7. Bornovas, J. (1974). Note on the Seismotectonics of Greece. In Proc. of the seminar on the seismotectonic map of the Balkan Region, Dubrovnik 1973, UNESCO, Skopje.

8. Doutsos, T., Kontopoulos, N. & Poulimenos, G. (1988). The Corinth – Patras rift as the initial stage of continental fragmentation behind an active island arc (Greece). *Basin Res*.1, 177 – 190.

9. Kiratzi, A., Sokos, E., Gans, A., Tselentis, A., Benetatos, C., Roumelioti, Z., Serpetsidaki, A., Andriopoulos, G., Galanis, O. & Petroucet, P. (2008). The April 2007 earthquake swarm near Lake Trichonis and implications for active tectonics in western Greece. *Tectonophysics*. 452 (1-4), 51-65.

10. Fotiadis, A. & Zananiri, I. (2015). Digitized Geological map of Greece in accordance with OneGeology standards. IGME-GR, Greek Geological Survey.

11. Corominas, J., van Westen, C., Frattini, L., Malet, J.-P., Fotopoulou, S., Catani, F., Van Den Eeckhaut, M., Mavrouli, O., Agliardi, F., Pitilaki, K., Winter, M.G., Ferlisi, S., Tofani, V., Hervas, J. & Smith, J.T. (2013). Recommendations for the quantitative analysis of landslide risk. *Bulletin of Engineering Geology and the Environment*. 73 (2), pp 209-263.

12. Cigna, F., Bianchini, S. & Casagli, N. (2012). How to assess landslide activity and intensity with Persistent Scatterer Interferometry (PSI): the PSI-based matrix approach. *Landslides* (10), 267–283.

13. Righini, G., Pancioli, V. & Casagli, N. (2012). Updating landslide inventory maps using Persistent Scatterer Interferometry (PSI). *International Journal of Remote Sensing*, 33 (7), 2068-2096.

14. Hooper, A., P. Segall, and H. Zebker (2007), Persistent Scatterer InSAR for Crustal Deformation Analysis, with Application to Volcán Alcedo, Galápagos, *J. Geophys. Res.*, 112, B07407.

15. Ferretti, A., Prati, C. & Rocca, F. (2001). Permanent scatterers in SAR interferometry. *IEEE Trans. Geosci. Remote Sens.*, 39 (1), 8–20.

16. Berardino, P., Fornaro, G., Lanari, R. & Sansosti, E. (2002). A new algorithm for surface deformation monitoring based on small baseline differential SAR interferograms. *IEEE Trans. Geosci. Remote Sens.*, 40 (11), pp. 2375–2383.

17. Hooper, A. (2008). A multi-temporal InSAR method incorporating both persistent scatterer and small baseline approaches. *Geophysical Research Letters*, 35, L16302.

18. Yin, K. J. & Yang T. Z. (1988). Statistical prediction model for slope instability of metamorphosed rocks. *In Proc. 5th. International Symposium on Landslides*, Lausanne, Switzerland, Vol. 2, pp. 1269-1272.

19. Zacharias, I., Dimitriou, E. & Koussouris, T. (2005). Integrated water management scenarios for wetland protection: application to Trichonis Lake. *Environmental Modelling and Software* 20, 177–185.

20. Vassilakis, E., Royden, L. & Papanikolaou, D. (2011). Kinematic links between subduction along the Hellenic trench and extension in the Gulf of Corinth, Greece: A multidisciplinary analysis. *Earth and Planetary Science Letters* (303), 108–120.

21. Stiros, S., Pytharouli, S., Kontogianni, V. & Psimoulis, P. (2008). In Proc. 1st Hellenic Conference on Large Dams, Larisa, Greece.